INORGANIC CHEMISTRY
FRONTIERS

RESEARCH ARTICLE

View Article Online
View Journal | View Issue

Cite this: *Inorg. Chem. Front.*, 2018, **5**, 643

Highly selective electrochemical detection of antipsychotic drug chlorpromazine in drug and human urine samples based on peas-like strontium molybdate as an electrocatalyst†

Jeyaraj Vinoth Kumar,[a] Raj Karthik,[b] Shen-Ming Chen, *[b] Thangavelu Kokulnathan, [b] Subramanian Sakthinathan, [c] Velluchamy Muthuraj,[a] Te-Wei Chiu [c] and Tse-Wei Chen[b]

The countless use of antibiotics in veterinary and human medicine causes severe health risks to both humans and animals. In this context, monitoring of the antibiotic drug in the veterinary and human pathological system is important and provokes a universal challenge. Therefore, development of simple and sensitive inorganic materials with unique morphology is of great importance for the trace level monitoring of pharmaceutical content in the environment. Herein, we developed a novel peas-like strontium molybdate catalyst ($SrMoO_4$; SrM) synthesized by a simple sonochemical approach and utilized as an electrochemical sensor for the detection of antipsychotic drug chlorpromazine (CPZ). The crystalline structure, surface morphology, elemental compositions and textural properties were systematically investigated by various analytical and spectroscopic techniques. As an electrochemical sensor, inorganic binary SrM modified screen printed carbon electrode (SrM/SPCE) exhibited an enhanced electrocatalytic activity towards CPZ sensing with excellent analytical performance such as wide linear response ranges and lowest detection limit of 0.1–143 and 153–1683 μM and 0.028 μM respectively. Moreover, the as-prepared SrM/SPCE showed an excellent selectivity even in the existence of co-interfering drugs, biological compounds and common metal ions. In addition, the SrM/SPCE applied to the real samples analysis in commercially available CPZ drug and human urine samples and the observed recoveries are quite satisfactory.

Received 23rd November 2017,
Accepted 6th January 2018

DOI: 10.1039/c7qi00743d

rsc.li/frontiers-inorganic

1. Introduction

Recently, inorganic binary metal oxides have been widely focused on by the researchers owing to their excellent electrical conductivity and superior electrochemical and photochemical behavior compared to single metal oxides.[1] Fascinatingly, molybdates combined with divalent metal cations possess great applications in the field of photoluminescence,[2] scintillators,[3] humidity sensors,[4] microwave devices[3] and energy storage devices.[5] In recent years, strontium molybdate ($SrMoO_4$) has been reported as one of the important inorganic alkaline-earth molybdates and widely utilized in the area of luminescent materials, photocatalysts, LED devices, solid state lasers, Raman scattering devices and quantum cutting materials due to their peculiar thermal and chemical stability, low phonon energy, high irradiation damage resistance and moisture-free properties.[6–11] In order to enhance the physicochemical properties of $SrMoO_4$, few reports have been published based on $SrMoO_4$ designed with different morphologies including nanocrystals, spindle-like, flower-like, dumbbell-like, nanowires, nanosheets, nanoplates, broccoli-like, nanoceramics, rice-like, peanut-like, and nanoparticles using different synthesis techniques, such as microwave irradiation, sol–gel, hydrothermal, co-precipitation and electrochemical process.[12–19] Very recently, our research group synthesized seed-like $SrMoO_4$ by simple precipitation route and utilized it as a photocatalyst and electrocatalyst towards post-harvest scald inhibitor diphenylamine.[20] Instead of these aforesaid methods, sonochemical technique can provide a simpler process and short reaction

[a]*Department of Chemistry, VHNSN College, Virudhunagar-626001, Tamil Nadu, India*
[b]*Electroanalysis and Bioelectrochemistry Lab, Department of Chemical Engineering and Biotechnology, National Taipei University of Technology, No. 1, Section 3, Chung-Hsiao East Road, Taipei 106, Taiwan, Republic of China.*
E-mail: smchen78@ms15.hinet.net; Fax: +886 2270 25238; Tel: +886 2270 17147
[c]*Department of Materials and Mineral Resources Engineering, National Taipei University of Technology, No. 1, Section 3, Chung-Hsiao East Road, Taipei 106, Taiwan, Republic of China*

†Electronic supplementary information (ESI) available. See DOI: 10.1039/c7qi00743d

time; also, this technique does not require high temperature and pressure. The resultant particles were of high uniformity, purity and homogenity.[21,22] Recently, J. Zhang *et al.* reported the fabrication of 3D sphere-like flower $SrMoO_4$ microarchitectures by adjusting the solution pH using sonochemical route and investigated its optical and photoluminescence properties.[23] Inspired by the aforementioned studies, we tried to fabricate peas-like $SrMoO_4$ using simple straight-forward sonochemical route and employed it as an electrochemical sensor for the sensitive and selective electrochemical detection of antipsychotic drug chlorpromazine (CPZ).

Chlorpromazine (3-(2-chloro-10*H*-phenothiazin-10-yl)-*N*,*N*-dimethyl-propan-1-amine) is an important antipsychotic drug in the group of phenothiazine derivatives with an aliphatic side chain.[24] CPZ is generally used for the treatment of personality and various mental disorders such as antihistaminic, anticholinergic and antipsychotropic diseases. In addition, CPZ is applied to control excitement, hyperkinetic states and aggression, psychomotor disturbances in schizophrenic patients, agitation, anxiety, tension and reduce the manic phase of manic depressive conditions.[25] Furthermore, CPZ is applied in palliative care to act as an anti-emetic drug[26] and also it works on a variety of receptors in the central nervous system to produce strong adrenolytic, spasmolytic, antiemetic, anticholinergic, hypothermic, hypotensive, antihistaminic and anesthetic effects. However, the overdose of CPZ or over usage can cause some severe health risks (main possible risk is cancer) to humans and the possible health risks have been well discussed and reported previously.[27] Therefore, a selective and sensitive technique is necessary to determine CPZ in biological fluid samples. Up to now, a number of analytical and spectroscopic techniques have been developed and utilized for accurate level detection of CPZ, including HPLC with UV detector, gas chromatography, spectrofluorimetry, flow injection, HPLC, potentiometry, spectrophotometry, electrochemiluminescence and capillary zone electrophoresis.[28–36] However, the aforementioned techniques provided accurate detection and good sensitivity towards CPZ, but they required sophisticated instruments and special training; also, these techniques are time consuming and require huge amount of reagents. Instead of these, voltammetric techniques have attracted more attention for biological, environmental and pharmaceutical analysis due to their high selectivity, rapid response, facile operation, simplicity, portability, good sensitivity and low cost procedure.[37–44]

In this study, we developed a facile, fast, cost-effective and stabilizing/reducing agent-free sonochemical approach for the synthesis of peas-like SrM. The as-prepared peas-like SrM was characterized by various spectroscopic and analytical techniques such as XRD, Raman, SEM, EDX, XPS, and BET, while the electrochemical properties were evaluated using voltammetry techniques. Peas-like SrM modified screen printed carbon electrode (SPCE) exhibited an excellent electrocatalytic activity for the electro-oxidation of CPZ. The prepared SrM modified SPCE are low-cost, reproducible, and disposable and demonstrate good electrocatalytic activity and high selectivity towards CPZ detection.

2. Experimental section

2.1. Materials and methods

Strontium nitrate ($Sr(NO_3)_2$), sodium molybdate (Na_2MoO_4), chlorpromazine ($C_{17}H_{19}ClN_2S$) and all other chemicals were purchased from Sigma-Aldrich and used without further purification. The screen printed carbon electrode (SPCE) was received from Zensor R&D Co., Ltd, Taiwan. The phosphate buffer solution (PB solution, 0.05 M) was prepared by mixing monobasic sodium phosphate (NaH_2PO_4) and sodium hydrogen phosphate (Na_2HPO_4). All the reagents and solvents were of analytical grade and used without further purification. All the required solutions were prepared using double-distilled (DD) water.

2.2. Characterization

The powder X-ray diffraction analysis was probed using XRD (XPERT-PRO spectrometer, PANalytical B.V., The Netherlands) with Cu-Kα radiation (λ = 1.5406 Å). Raman spectrum of the sample was recorded using an NT-MDT, NTEGRA SPECTRA spectrometer. Scanning electron microscope (SEM) and Energy dispersive X-ray (EDX) results were obtained using Hitachi S-3000 H microscope (SEM Tech Solutions, USA) attached with HORIBA EMAX X-ACT. X-ray photoelectron spectroscopy (XPS) results were collected using Thermo ESCALAB 250 instrument. The Micromeritics, ASAP 2020M instrument was used to determine the specific surface area and pore size distribution of the material. All the electrochemical measurements were performed by cyclic voltammetry (CV) and differential pulse voltammetry (DPV) using CHI 405a and CHI 900 electrochemical workstation (CH Instruments Company, made in U.S.A) with a conventional three electrode cell system comprised of an SPCE as the working electrode (working area = 0.07 cm^2), platinum wire as the auxiliary electrode and Ag/AgCl (saturated KCl) as the reference electrode, respectively.

2.3. Preparation of peas-like SrM

In a typical synthesis, 2.06 g Na_2MoO_4 was dissolved in 50 mL DD water (0.2 M) and it was placed in an ultrasonic bath (300 W). Following this, 0.1 M $Sr(NO_3)_2$ (1.05 g in 50 mL DD water) was added to the above solution and the suspension was ultrasonicated for 30 min at room temperature (the obtained solution pH is 5). Consequently, the resultant white products were washed with DD water and acetone to remove the unwanted impurities, and dried at 60 °C overnight to eliminate the adsorbed hydrates. The overall synthesis procedure and the applications of peas-like SrM as shown in Scheme 1.

2.4. Fabrication of peas-like SrM modified electrode

Prior to the modification, the bare SPCE was washed with water and ethanol to remove impurities on the electrode surface. The peas-like SrM was dispersed in DD water at a concentration of 5 mg mL^{-1} and sonicated for 15 min to obtain a homogeneous suspension. About 8 μL (optimized concentration) of peas-like SrM suspension was drop coated on the SPCE surface, following which it was allowed to dry at room

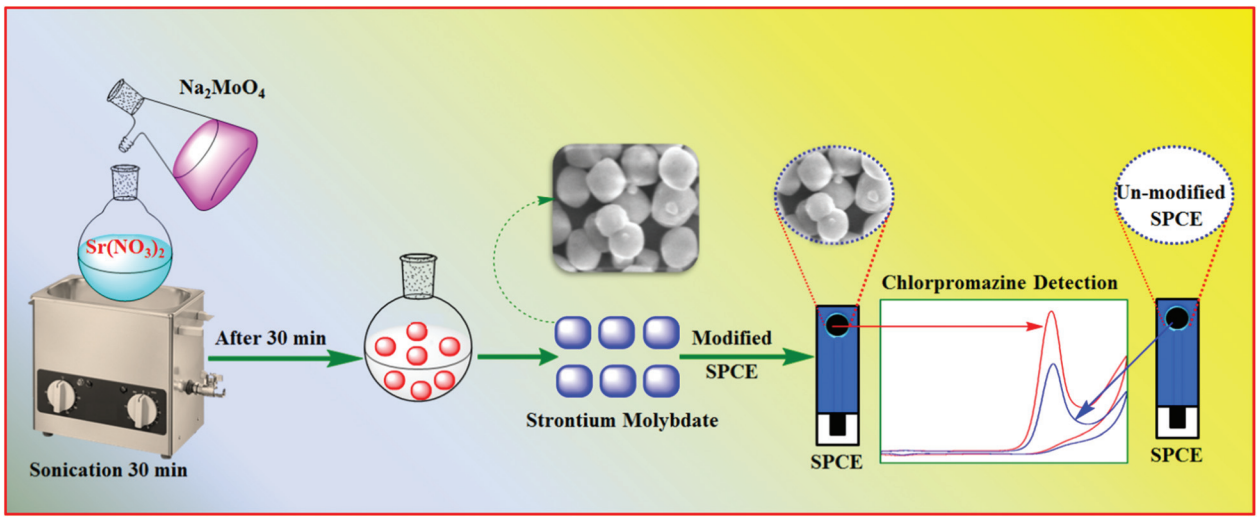

Scheme 1 The overall synthesis procedure of peas-like SrM and its electrochemical applications for the detection of CPZ.

temperature. Later, the dried SPCE was gently washed with DD water to remove loosely attached SrM on the SPCE surface. The obtained peas-like SrM modified SPCE was used for further electrochemical measurements.

3. Results and discussion

3.1. Characterization of peas-like SrM

The crystallographic nature of the as-prepared material was analyzed by XRD technique. Fig. 1A depicts the XRD pattern of the as-prepared SrM, which displayed the peaks at 2θ = 18.01, 27.6, 29.7, 33.1, 38.1, 45.14, 47.6, 51.5, 55.9, 57.1, 72.7, 72.9, 76.52, 77.5, and 79.3° were attributed to the (101), (112), (004), (200), (114), (204), (220), (116), (312), (224), (136), (109), (332), (404) and (240) miller indices planes of tetragonal $SrMoO_4$ and the results are accurately matched with their standard JCPDS file no. 85-0809. No other noticeable peaks were observed, implying the good crystalline nature of $SrMoO_4$. From the XRD results, the average crystallite size was calculated using Scherer's formula,

$$D = (k\lambda/\beta \cos \theta) \quad (1)$$

where D is the crystallite size, λ is wavelength (1.541 Å), k is Scherer's constant (0.9), β is FWHM (full width at half maximum) of the (112) diffraction peak and θ is the diffraction angle. The average crystallite size of the as-prepared SrM is estimated to be 47 nm.

Raman spectrum (Fig. 1B) demonstrates that the high intense peaks at 890 and 320 cm^{-1} were attributable to the

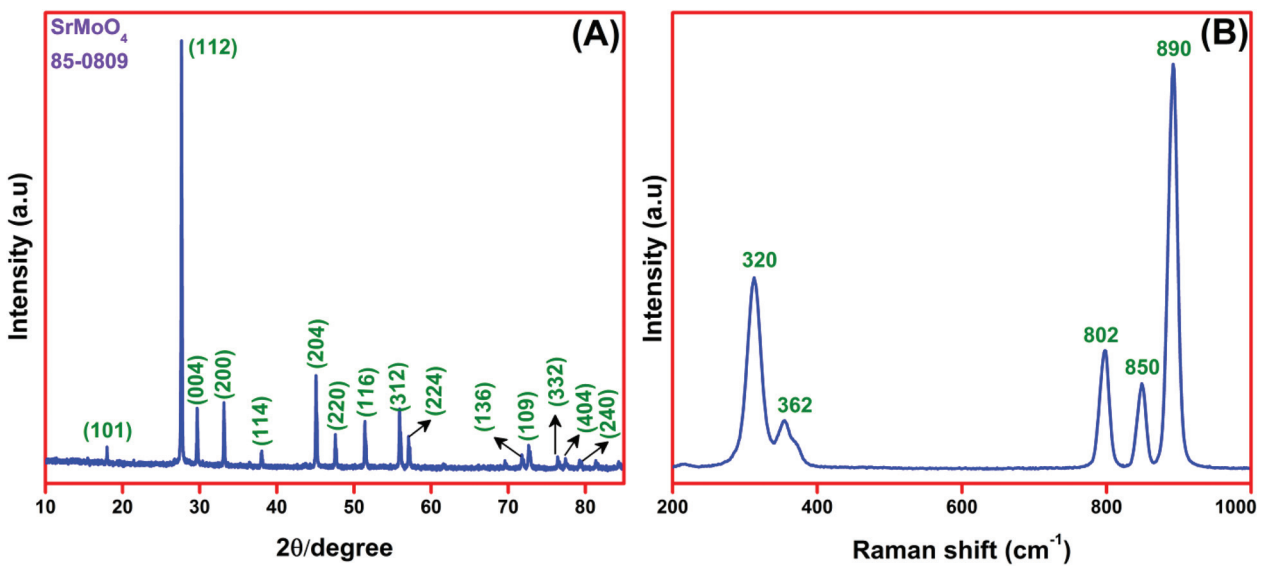

Fig. 1 XRD pattern (A) and Raman spectrum of peas-like SrM (B).

symmetric stretching ν_1 (A_g) and symmetric bending ν_2 (A_g) vibrations of MoO_4^{2-} tetrahedron in $SrMoO_4$, respectively. In addition, the weak peaks at 850, 802 and 362 cm^{-1} were attributed to the ν_3 (B_g) and ν_3 (E_g) asymmetric stretching vibrations and ν_4 (B_g) asymmetric bending vibrations, respectively.[45] The XRD and Raman results clearly suggested the presence of single-phase $SrMoO_4$ without any other significant impurities. The surface topology of the as-prepared $SrMoO_4$ was investigated by SEM studies. Fig. 2(A–C) clearly show the peas-like structure of SrM, in which the "peas" are attached to one another at their ends. The elemental composition of the as-prepared SrM was determined by EDX analysis and shown in Fig. 2D. It clearly demonstrated that the peas-like $SrMoO_4$ could be composed of Sr, Mo and O elements with the quantitative ratio of 1 : 1 : 4 (insert: Fig. 2D), respectively, which is in good consistence with the experimental protocols. In addition, the elemental mapping result (Fig. 3(B–D)) corroborates that the Sr (red color), Mo (green color) and O (blue color) elements have the uniform peas-like shape and size at their selected scanning region (Fig. 3A).

XPS is one of the most sensitive tools to predict the elemental compositions and the exact electronic states of the as-prepared peas-like $SrMoO_4$ and the results are documented in Fig. 4. As shown in Fig. 4A, the overall XPS survey spectrum of $SrMoO_4$ comprises of Sr 3d, C 1s, Mo 3d and O 1s peaks, which is in good agreement with the EDS results. The additional C 1s peak arises from the survey spectrum due to the adventitious hydrocarbon contained in the instrument. The enlarged Sr 3d XPS spectrum (Fig. 4B) depicts the Sr $3d_{5/2}$ and Sr $3d_{3/2}$ spin-orbits centered at 133.3 and 134.8 eV, respectively, which revealed that Sr is present in divalent oxidation state in $SrMoO_4$.[46] The XPS spectrum in Fig. 4C portrays the doublet peaks appearing at 232.8 and 235.7 eV, representing the Mo $3d_{5/2}$ and Mo $3d_{3/2}$ core-levels, which ascribe to the Mo^{6+} state.[47] The high magnification O 1s (Fig. 4D) spectrum depicts that the peaks at the binding energies of 530.5, 531.3 and 532.1 eV are ascribed to the O^{2-} state of lattice oxygen, defect and adsorbed oxygen species, respectively.[48] The obtained XPS results confirmed that the phase structure of $SrMoO_4$ are composed of +2, +6 and −2 valence states of Sr, Mo and O elements, respectively. Fig. 5A represents the N_2 adsorption/desorption isotherm and its corresponding pore size distribution of peas-like SrM. As shown in Fig. 5A, the determined BET specific surface area of the SrM is 11.8 $m^2\ g^{-1}$

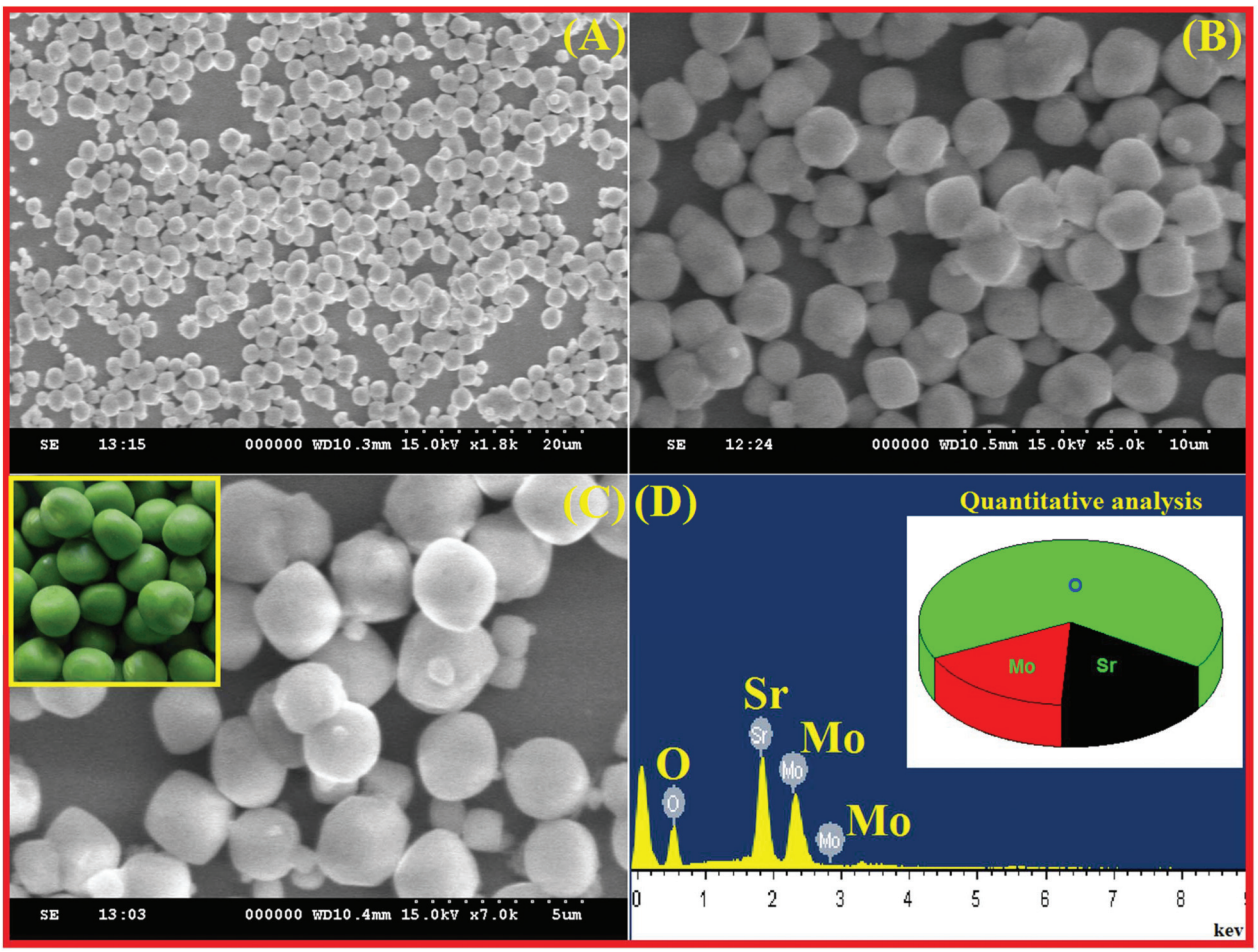

Fig. 2 Different magnification SEM micrographs of peas-like SrM 20 μm (A), 10 μm (B) 5 μm (C) and their corresponding EDX spectrum (D). Inset: Quantitative analysis of as-prepared peas-like SrM.

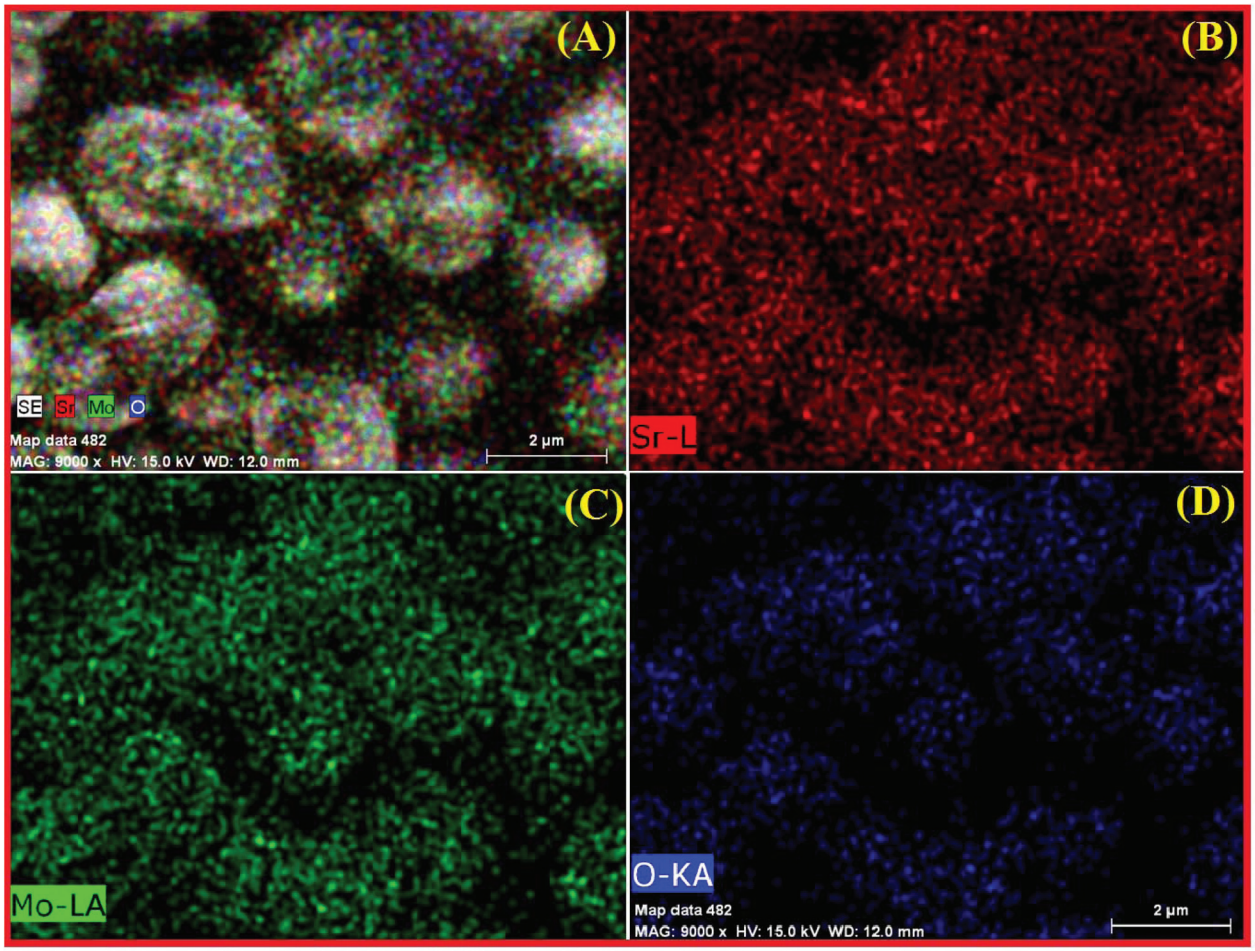

Fig. 3 The SEM image and EDX elemental mapping image of SrM (A) and individual mapping images of Sr (B), Mo (C) and O (D) elements.

and their average pore size distribution (Fig. 5B) was derived from Barrett–Joyner–Halenda (BJH) method, which demonstrated the mesoporous range of 8 nm. The sharp and constricted pore size distribution revealed the uniform nature of the mesopores.

3.2. Electrochemical characterization of bare SPCE and peas-like SrM/SPCE

CV was used to study the electrochemical properties of the bare SPCE and peas-like SrM modified SPCE in $[Fe(CN)_6]^{3-/4-}$ solution to prove their redox nature. Fig. 6A shows the electrochemical responses attained by CV between −0.5 and +0.8 V (*vs.* Ag/AgCl) at bare SPCE and SrM/SPCE measured in 0.1 M KCl solution containing 5 mM $[Fe(CN)_6]^{3-/4-}$ (5 : 5) at 50 mV s^{-1}. The ratio between cathodic and anodic peaks was around 1 for both bare SPCE and SrM/SPCE, indicating the reversibility of the system. At bare SPCE (curve a), well-defined redox (oxidation and reduction) peaks were observed with peak currents of I_{pa} = 49 and I_{pc} = 45 μA. When the bare SPCE was modified with peas-like SrM (curve b), a slight decrease in peak potential and an evident increase in both peak currents were observed with peak currents of I_{pa} = 73 and I_{pc} = 70 μA, which suggests that the electron transfer rate at peas-like SrM modified SPCE was improved. The CV scans were recorded on the SrM/SPCE surface at various scan rates. The process on the surface of SrM/SPCE was studied in the same solution of 5 mM $[Fe(CN)_6]^{3-/4-}$ in the different scan rate ranging from 10–100 mV s^{-1} and is displayed in Fig. 6B. From Fig. 6B, it can be clearly observed that the noteworthy increment in both peak currents was obtained with an increase in the scan rate. The linear plot was obtained by plotting the square root of scan rate *vs.* peak current (inset of Fig. 6B) with a linear regression equation as follows:

$$I_p\ (\mu A) = 9.200\ (\nu^{1/2}, \text{mV s}^{-1}) + 7.385;\ R^2 = 0.9995 \quad (2)$$

The active surface areas for SrM/SPCE and bare SPCE were determined using the $[Fe(CN)_6]^{3-/4-}$ redox system and the electrode active area was calculated using the Randles–Sevcik equation:[49]

$$I_p = (2.69 \times 10^5) n^{3/2} A C D^{1/2} \nu^{1/2} \quad (3)$$

where, ν is the scan rate (V s^{-1}), D is the diffusion coefficient of $[Fe(CN)_6]^{3-/4-}$ in solution (cm^2 s^{-1}), C is the concentration of $[Fe(CN)_6]^{3-/4-}$ (mol L^{-1}), A is the electrode area (cm^2) and n

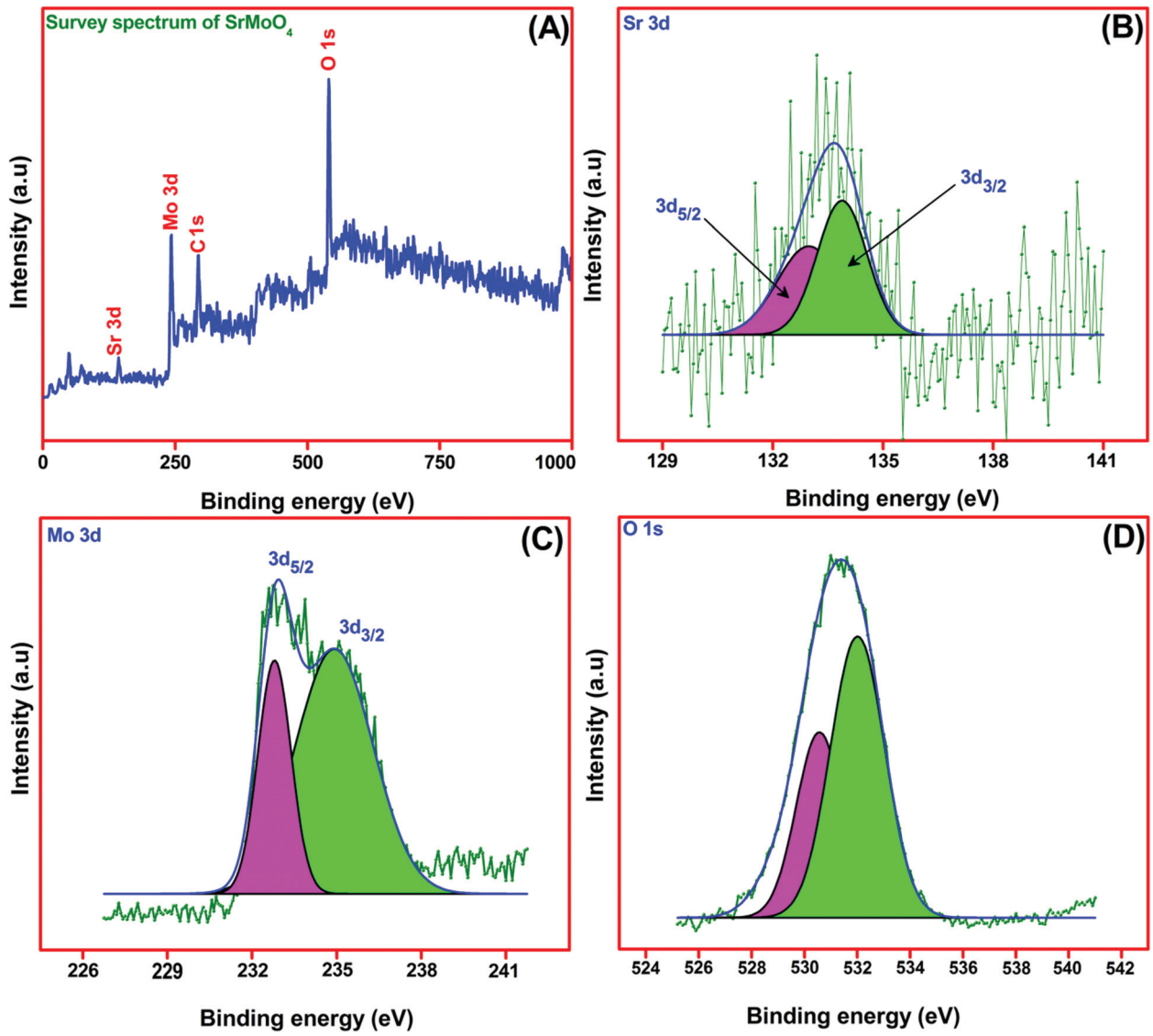

Fig. 4 XPS survey spectrum of peas-like $SrMoO_4$ (A) and high magnification XPS spectra of Sr 3d (B), Mo 3d (C) and O 1s (D).

is the number of electrons. The active areas for SrM/SPCE and bare SPCE were calculated as 0.054 and 0.039 cm^2, respectively. These results prove that the peas-like SrM has the largest active surface area, which is very helpful in improving the electrocatalytic activity for the detection of CPZ.

3.3. Evaluation of electrocatalytic activity at SrM modified SPCE towards CPZ

The peak current and sensitivity of the electrode could be directly affected by the larger/fewer amount of catalyst loading on the electrode surface. Therefore, we investigated the influence of the loading level such as 4, 6, 8, and 10 μL of peas-like SrM on the SPCE in the presence of 200 μM CPZ containing 0.05 M PB solution (pH 7) at a scan rate of 50 mV s^{-1} as shown in Fig. 7A. From Fig. 7A, it can be clearly observed that the electrochemical oxidation peak current of CPZ gradually increases on increasing the loading level of SrM/SPCE up to 8 μL. Beyond that (above 8 μL), the oxidation peak current decreased, which clearly suggests that the limited quantity (loading level is 8 μL SrM/SPCE) of SrM modified SPCE can effectively catalyze the CPZ. Therefore, the 8 μL of peas-like SrM drop casted modified SPCE was chosen for further electrochemical studies towards CPZ sensing.

3.4. Electrochemical behavior of CPZ at peas-like SrM modified electrode

The electrochemical oxidation behavior of CPZ at various modified and unmodified electrodes was studied by CV as shown in Fig. 7B. The CV responses of the unmodified SPCE (bare SPCE) (Fig. 7B(b)) and peas-like SrM modified SPCE (Fig. 7B(a)) in the presence (c, d) and absence (a, b) of 200 μM antipsychotic drug CPZ were obtained in 0.05 M PB (pH 7) solution at a scan rate of 50 mV s^{-1} and the selected potential window ranging from 0 to 1 V. From Fig. 7B(a, b), it can be

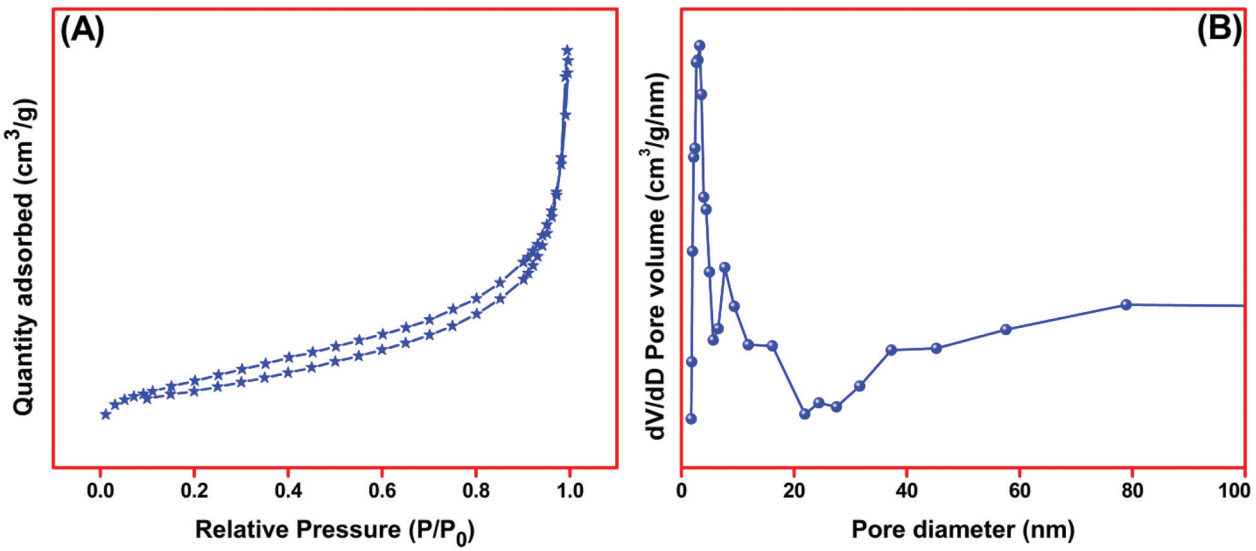

Fig. 5 BET nitrogen adsorption/desorption isotherms (A) and their corresponding BJH pore size distribution (B) of peas-like SrM.

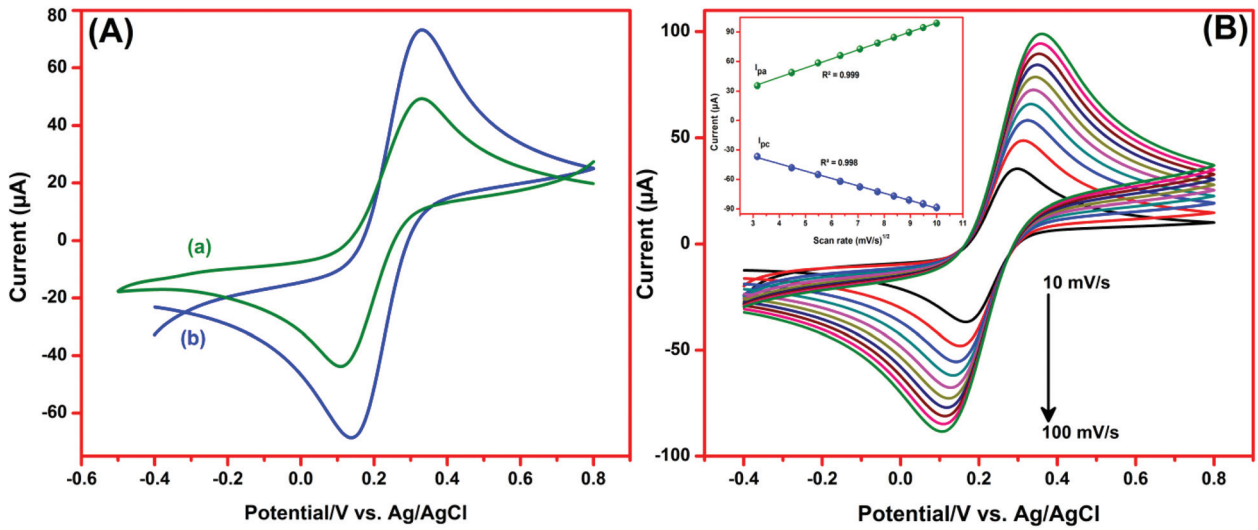

Fig. 6 CVs of unmodified and modified electrodes in 5 mM $[Fe(CN)_6]^{3-/4-}$ containing 0.1 M KCl at 50 mV s^{-1}; bare SPCE (a) and SrM/SPCE (b) (A). CVs of the SrM/SPCE in 5 mM $[Fe(CN)_6]^{3-/4-}$ containing 0.1 M KCl at scan rates 10–100 mV s^{-1}. Insert: Linear plot for redox (I_{pa} and I_{pc}) peak current *vs.* square root of scan rate (B).

observed that no visible electrochemical oxidation peak was observed when the PB solution had no CPZ. Subsequently, the sharp and well-defined irreversible oxidation peak current was observed at the potential of +0.7 V (bare SPCE; Fig. 7B(c)) and +0.68 V (peas-like SrM/SPCE; Fig. 7B(d)) when CPZ (200 μM) was added into the PB solution (pH 7). The peas-like SrM modified SPCE shows higher oxidation peak current in the presence of 200 μM CPZ at lower positive potential when compared to bare SPCE, which indicates that peas-like SrM/SPCE has excellent detection capability towards CPZ sensing. Moreover, the obtained oxidation peak current is 0.6-fold higher when compared to bare SPCE. Furthermore, the irreversible oxidation peak appeared at 0.68 V, which is due to the direct oxidation of nitrogen atom in the CPZ.[50] The possible electrochemical oxidation mechanism of CPZ at SrM/SPCE is shown in Scheme 2. The enhanced electrochemical activity of peas-like SrM modified SPCE for the detection of CPZ may be due to the availability of large surface area on the SrM surfaces, which is very helpful to improve the catalytic activity and act as an excellent electron mediator for the CPZ sensing. Furthermore, the peas-like SrM offers an ultrafast charge carrier and charge transfer; the relay of electron transfer is very efficient and rapid. In addition, the particular alignment of conduction and valence band of the SrM favors electron transfer towards the oxidation of CPZ and forms the oxidized product.

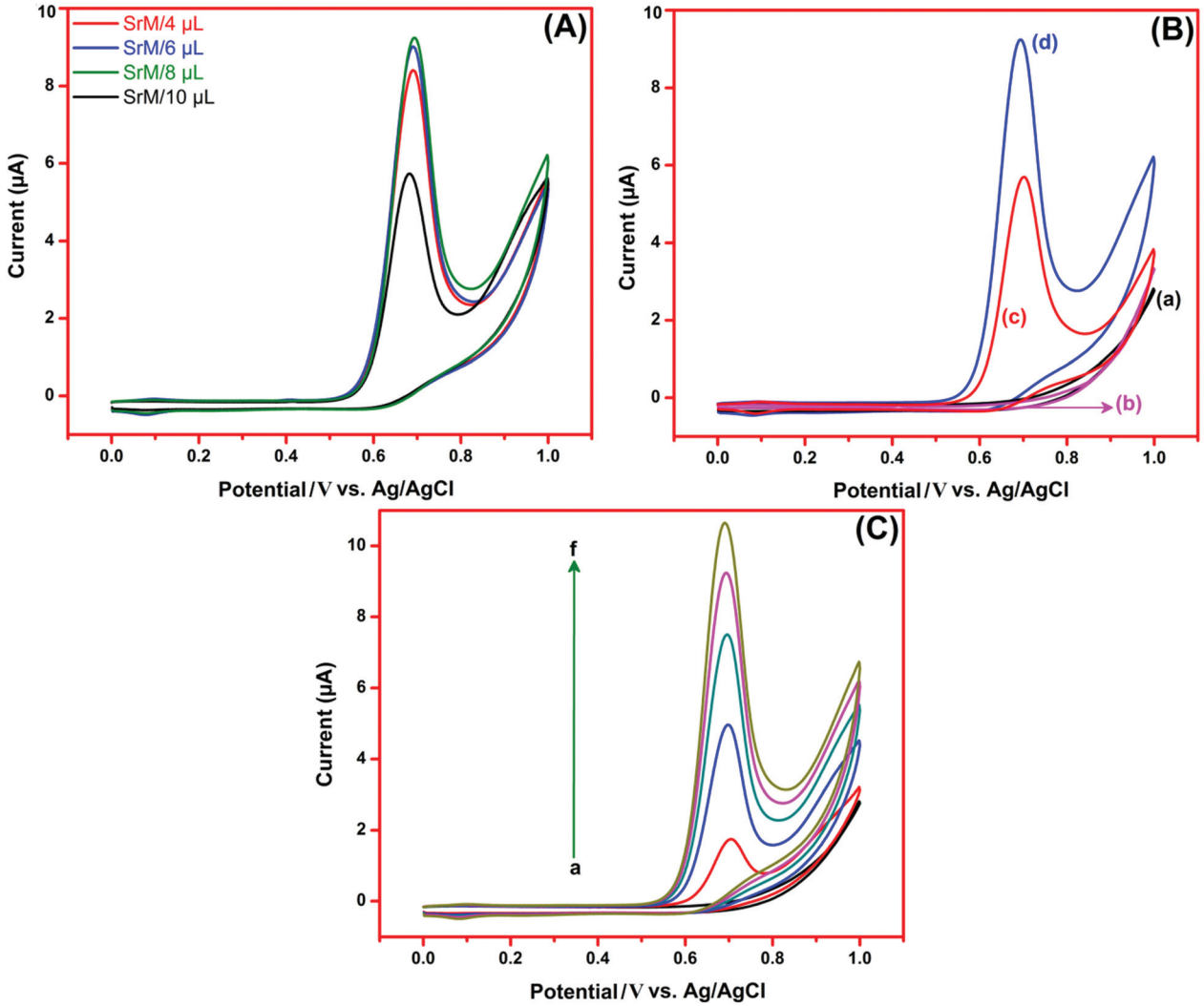

Fig. 7 CVs response of CPZ (200 µM) with various loading levels of SrM on the SPCE (A). CVs obtained at (a) peas-like SrM modified SPCE and (b) bare SPCE (absence of 200 µM CPZ) and presence of 200 µM CPZ, (c) bare GCE and (d) peas-like SrM/SPCE in PB solution (pH 7) at scan rate of 50 mV s^{-1} (B). CVs recorded for peas-like SrM/SPCE in the absence (a) and presence of different concentration of CPZ (0–250 µM); (a–f) in the 0.05 M PB solution (C).

Moreover, the electrocatalytic activity was examined at peas-like SrM modified SPCE in the absence and presence of various concentrations of CPZ ranging from 0 to 250 µM (0–250; a–f) containing 0.05 M PB solution (pH 7) at a scan rate of 50 mV s^{-1} (Fig. 7C). This clearly shows that the oxidation peak current gradually increases with an increase in the concentration of antipsychotic drug CPZ from 50 to 250 µM, which clearly indicates that the peas-like SrM modified SPCE has higher electrocatalytic activity towards the CPZ drug sensing. In addition, the peas-like structure of SrM has a large surface area and it could act as a good adsorbent to adsorb all quantities of CPZ molecules, which could then be oxidized by SrM, leading to the drastic increase in the electrocatalytic activity for the detection of CPZ. Hence, we found that the peas-like SrM modified SPCE is a more active and suitable electrode material for the electrochemical oxidation of antipsychotic drug CPZ. DPV technique was further utilized for the highly sensitive sensing of CPZ at peas-like SrM modified SPCE.

3.5. Influence of scan rates and pH

Fig. 8A reveals the CVs of peas-like SrM modified SPCE at various scan rates (20–180 mV s^{-1}; a–j) in 0.05 M PB solution (pH 7) containing 200 µM of CPZ. Fig. 8A shows that on increasing the scan rate from 20 to 180 mV s^{-1}, the oxidation peak current of CPZ increased linearly. Furthermore, the oxidation peak potential of the CPZ was also shifted towards the more positive potential side by increasing the scan rate from 20 to180 mV s^{-1}. A linear relationship was obtained between the oxidation peak current and scan rate (the linear regression equation of I_{pa} (µA) = 0.183 (mV s^{-1}) + 1.845 with a correlation coefficient of R^2 = 0.9947) as depicted in Fig. 8B, which indi-

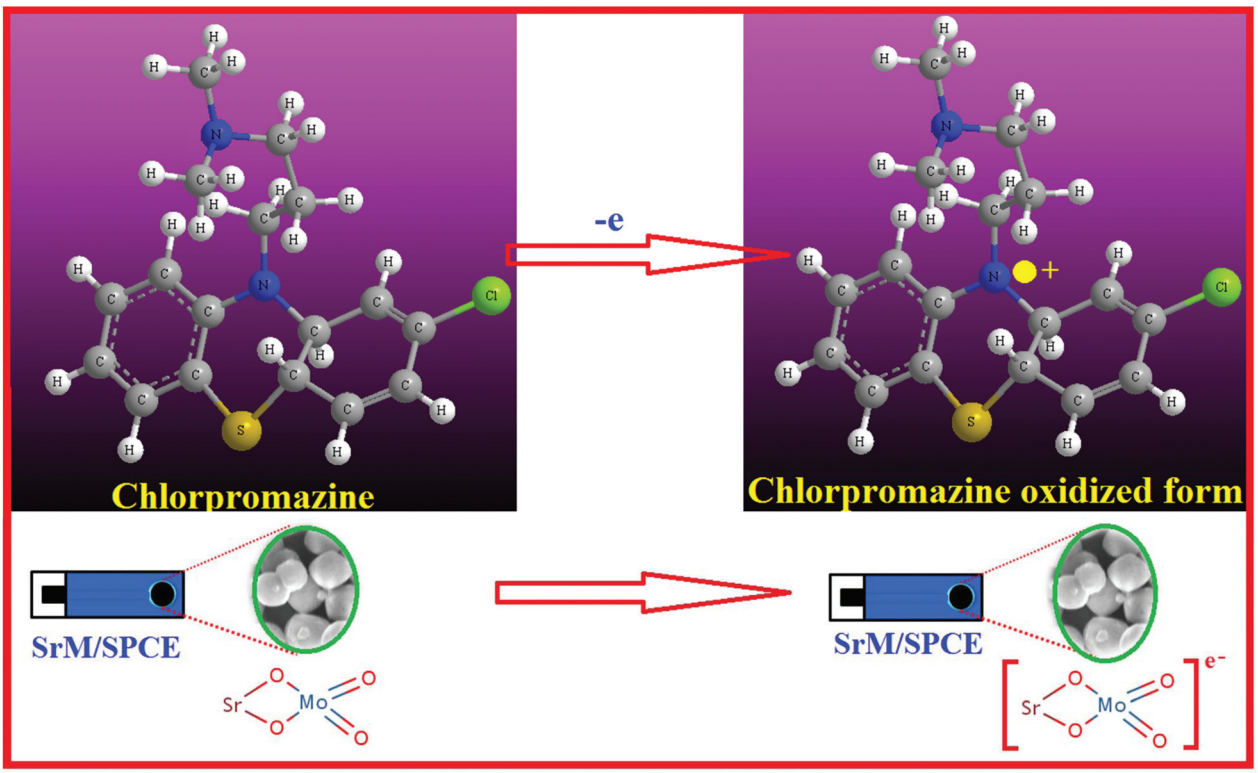

Scheme 2 The overall electrochemical oxidation mechanism of CPZ on the SrM modified SPCE.

cates that the oxidation process of CPZ at the peas-like SrM modified SPCE is an adsorption-controlled process.

In electrochemical studies, the peak shape, current and potential of the CVs might change on changing the pH of the electrolyte, which can affect the electrochemical response of CPZ. Therefore, we investigated the influence of pH on the electrochemical performance of CPZ (200 μM) at peas-like SrM modified SPCE by CVs in the pH range of 3–11 at a scan rate of 50 mV s^{-1} (Fig. 8C). The oxidation peak current of CPZ gradually increased with the increase in pH up to 7 (Fig. 8C, right to left direction) and the oxidation peak current gradually decreased with the increase in pH above 7. Fig. 8D shows the calibration plot for the oxidation peaks observed in Fig. 8C, which confirms that the maximum oxidation peak current of CPZ was observed at pH 7. Hence, 0.05 M PB solution (pH 7) was utilized as the favorable electrolyte for the further electrochemical measurements towards CPZ sensing.

3.6. Determination of CPZ at peas-like SrM modified SPCE

For the determination study, differential pulse voltammetry (DPV) technique was utilized to determine the CPZ due to their better selectivity, high sensitivity and better resolution techniques when compared with conventional CVs and the obtained results are displayed in Fig. 9A. It can be clearly observed that the response of the sensor for the oxidation peak current of CPZ gradually increases with an increase in the concentration of CPZ from lower to higher (0.1–1683 μM), which suggests that the as-proposed SrM modified SPCE has excellent electrocatalytic activity for the detection of CPZ drug. The calibration plot was plotted between the CPZ concentration and oxidation peak current. As a result, two linear ranges were observed from the lower and higher concentration of CPZ (Fig. 9B). The first linear range is from 0.1 to 143 μM (lower concentration range) with the linear regression equation of I_{pa} (CPZ) = 0.0832C + 0.5436 and the correlation coefficient of R^2 = 0.9964, the second linear range is from 153 to 1683 μM (higher concentration range) with the linear regression equation of I_{pa} (CPZ) = 0.0231C + 11.27 and the correlation coefficient of R^2 = 0.9927. The limit of detection (LOD) and sensitivity of the peas-like SrM modified SPCE towards CPZ was calculated from the lower linear response range, which are 0.028 μM and 1.18 μA μM^{-1} cm^{-2}, respectively. Moreover, the acquired analytical parameters such as sensitivity, wide linear response range and LOD of the peas-like SrM modified SPCE towards CPZ was compared with previously reported CPZ sensor and listed in Table 1. As summarized in Table 1, we achieved very low LOD, wide linear response ranges and good sensitivity compared with other reported CPZ sensor. To the best of our knowledge, there is no report available in literature concerning the use of modified electrodes with peas-like SrM for the determination of CPZ. The lower detection limit and higher electrocatalytic activity towards CPZ at SrM modified SPCE could be attributed to the availability of large surface area, which helps in improving the electrocatalytic activity and adsorbing the target analyte on the surface of SrM.

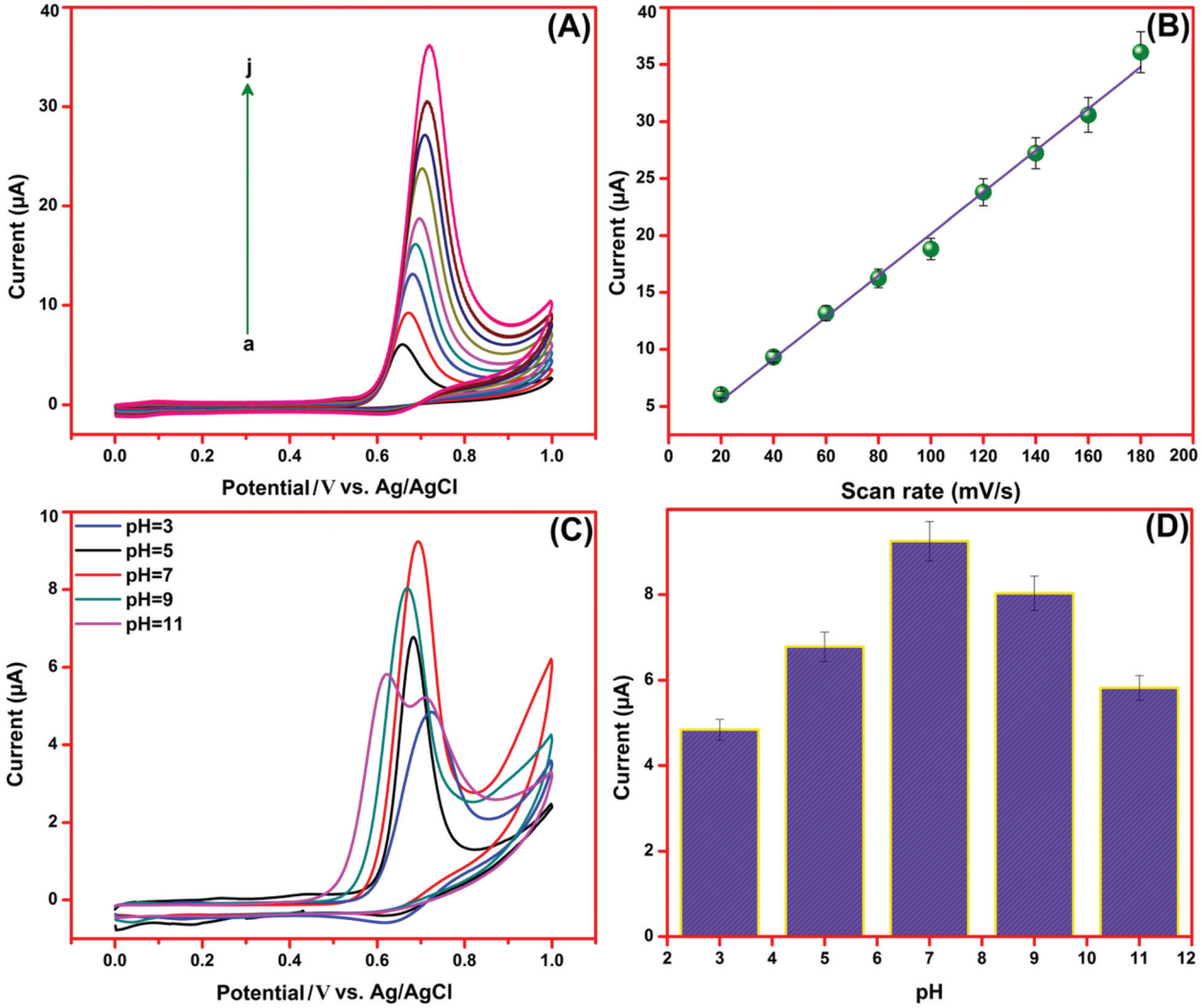

Fig. 8 CVs of 200 μM CPZ in PB solution (pH 7) at various scan rates 20–180 mV s^{-1} (a–j) at SrM/SPCE (A). A linear plot of anodic peak current *vs.* scan rate (B). CVs response for 200 μM CPZ at peas-like SrM/SPCE in various pH solutions from 3 to 11 at a scan rate of 50 mV s^{-1} (C). The calibration plot between anodic peak current *vs.* pH (D).

3.7. Selectivity of the sensor

Selectivity is a very significant parameter for the newly developed electrochemical sensor. To evaluate the selectivity of CPZ at peas-like SrM modified SPCE containing the interferences that potentially co-interfere with CPZ such as caffeic acid (CA), catechol (CC), hydroquinone (HQ), dopamine (DA), metronidazole (MTZ), riboflavin (RIB), uric acid (UA), chlorpheniramine maleate (CHL), glucose (GLU), amitrole (AMI), pyridoxine (PYR), ascorbic acid (AA), NO_2^-, K^+, Fe^{2+}, Ca^{2+}, Cu^{2+}, Ni^{2+}, Mg^{2+}, I^-, Br^-, Cl^-, and SO_4^- were selected for the interference studies. The CVs response of aforementioned interfering species and the peak current changes (relative error bar) are displayed in Fig. 9(C, D) and Fig. S2† (common metal ions). It can be clearly observed that the drugs, common metal ions and biological compounds such as CC, MTZ, RIB, CHL, GLU, AMI, PYR, AA, K^+, Fe^{2+}, Ca^{2+}, Cu^{2+}, Ni^{2+}, Mg^{2+}, I^-, Br^-, Cl^-, and SO_4^- have a negative interfering effect of ~1–10% on the CPZ detection. Moreover, the electrochemical oxidations of CPZ current response changed by ~2–8% in the presence of 10 fold excess concentration of CA, HQ, DA and NO_2^- (Fig. S2†). The obtained result revealed that the peas-like SrM modified SPCE is very suitable for the selective detection of CPZ even in the aforementioned biological compounds, common metal ions and drugs. Due to the excellent selectivity behavior of peas-like SrM, it can be used for the real sample analysis in pharmaceuticals and water samples.

3.8. Long-term stability and repeatability analysis of peas-like SrM/SPCE

The stability of the electrochemical response of peas-like SrM/SPCE was investigated by 15 consecutive DPV numbers in 0.05 M PB solution (pH 7) containing 70 μM CPZ. As shown in Fig. S1,† with the oxidation peak current of first cycle as the reference, after 15 cycles, the oxidation peak current slightly

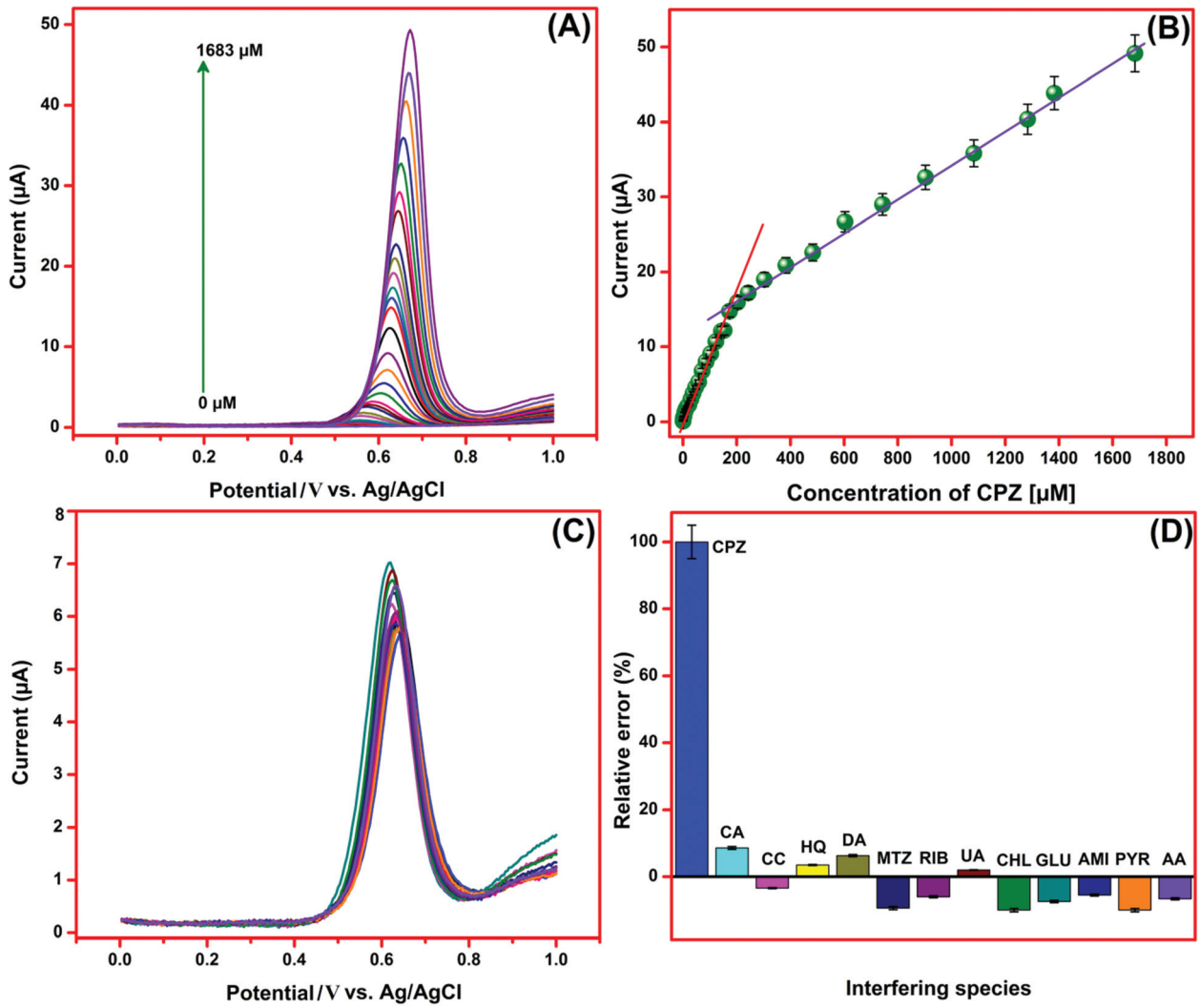

Fig. 9 DPV response of the peas-like SrM/SPCE to consecutive addition of CPZ from 0.1 to 1683 μM in 0.05 M PB solution (pH 7) (A). The calibration plot for the anodic peak current *vs.* concentrations of CPZ (B). The DPV responses of CPZ oxidation in the presence of co-interfering compounds; CA, CC, HQ, DA, MTZ, RIB, UA, CHL, GLU, AMI, PYR and AA (C). Relative error bar for the interfering species. The *x* axis indicates the tested interfering compounds and the *y* axis indicates interference effect in percentage (%) (D).

Table 1 The comparison of analytical performance of peas-like SrM modified SPCE with previously reported modified electrode for the detection of CPZ

Electrodes	Linear range (μM)	LOD (μM)	Ref.
PTN	0.1–130.0	0.03	51
P3MT/γ-CD/GCE	0.14–3.363	0.1	52
BDDE	0.1–40	0.03	53
GPE	0.01–9.00	0.006	54
CdO/NPs/IL/CPE	0.1–350	0.07	55
GCE	0.7–14	0.4	56
Ruthenium electrodes	200–800	—	57
Peas-like SrM/SPCE	0.1–143; 153–1683	0.028	This work

Abbreviation: PTN-polythiophene nanowires, P3MT/γ-CD-poly-3-methylthiophene-cyclodextrin, GCE-glassy carbon electrode, BDDE-boron-doped diamond electrode, GPE-graphene paste electrode, CdO-cadmium oxide, NPs-nanoparticles, IL/CPE-ionic liquid carbon paste electrode.

decreased, suggesting that the peas-like SrM modified SPCE has good long-term stability. The repeatability of the peas-like SrM modified SPCE was studied by CVs with 70 μM CPZ in 0.05 M PB solution (pH 7) for 10 consecutive measurements. The relative standard deviation (RSD) obtained was 2.45% in CPZ, which suggests the peas-like SrM modified SPCE had good repeatability of the sensor.

3.9. Analytical applications to commercial drug and human urine samples

The peas-like SrM modified SPCE was applied to the real sample analysis of CPZ in tablet and urine samples. The CPZ (WINSUMIN) (12.5 mg) tablet was directly purchased from the medical shop and the urine sample was collected from the healthy person. Before the real sample analysis, the CPZ stock solutions were prepared using PB solution and the known con-

Table 2 Results of determination of CPZ in drug and human urine samples

Sample	Added (μM)	Found (μM)	Recovery (%)
CPZ drug	0.0	—	—
	10.0	9.83	94.8
	20.0	19.96	99.8
Human urine	0.0	—	—
	10.0	9.97	99.7
	20.0	19.91	99.5

centration of CPZ spiked into the real sample. In addition, the urine sample was CPZ-free; therefore, known concentration of CPZ was spiked into the urine samples. Both the spiked samples were used for the real sample analysis. The experimental condition was followed as described in section 3.5. The spiked values and the obtained recovery results were calculated using standard addition method and the result is summarized in Table 2. From the result, the observed recovery values are 94.8–99.8%, suggesting that the peas-like SrM had great practical viability for the determination of CPZ in real sample analysis.

4. Conclusion

In summary, we successfully developed an inorganic binary peas-like SrM *via* simple sonication method without using any other surfactant. The as-prepared peas-like SrM was characterized by various spectroscopic and analytical techniques such as XRD, Raman, SEM, EDX, XPS and BET studies. The electrochemical properties of peas-like SrM were studied by different voltammetry techniques. Fascinatingly, the peas-like SrM showed an excellent electrocatalytic activity for the oxidation of CPZ. DPV determination of CPZ at the peas-like SrM exhibits lower detection limit, good sensitivity and wide linear response range. Furthermore, CPZ could be selectively determined in the presence of biological compounds, potentially interfering drugs and common metal ions using the SrM/SPCE. Furthermore, the SrM/SPCE was successfully applied to the real sample analysis in commercial tablet and urine sample and appreciable results were achieved. The proposed peas-like SrM modified SPCE offers a new window to detect CPZ selectively and sensitively in pharmaceutical analysis.

Conflicts of interest

There are no conflicts of interest to declare.

Acknowledgements

This project was supported by the Ministry of Science and Technology (MOST 106-2113-M-027-003 and MOST 106-2811-M-027-004), Taiwan, ROC.

References

1 Y. Zhang, L. Li, H. Su, W. Huang and X. Dong, *J. Mater. Chem. A*, 2015, **3**, 43–59.
2 J. P. Liu, X. T. Huang, Y. Y. Li and Z. K. J. Li, *J. Mater. Chem.*, 2007, **17**, 2754–2758.
3 J. H. Ryu, J. W. Yoon, C. S. Lim and K. B. Shim, *Key Eng. Mater.*, 2006, **317**, 223–226.
4 R. Sundaram and K. S. Nagaraja, *Sens. Actuators, B*, 2004, **101**, 353–360.
5 W. Xiao, J. S. Chen, C. M. Li, R. Xu and X. W. Lou, *Mater. Chem.*, 2010, **22**, 746–754.
6 D. Errandonea, R. S. Kumar, X. Ma and C. Tu, *J. Solid State Chem.*, 2008, **181**, 355–364.
7 G. Ahmad, M. B. Dickerson, B. C. Church, Y. Cai, S. E. Jones, R. R. Naik, J. S. King, C. J. Summers, N. Kroger and K. H. Sandhage, *Adv. Mater.*, 2006, **18**, 1759–1763.
8 X. Ma, J. Li, Z. Zhu, Z. You, Y. Wang and C. Tu, *J. Phys. Chem. Solids*, 2008, **69**, 2411–2415.
9 A. Kaminski, S. Bagaev, K. Ueda, K. Takaichi and H. Eichler, *Crystallogr. Rep.*, 2002, **47**, 653–657.
10 S. Y. Wu, H. N. Dong and W. H. Wei, *J. Alloys Compd.*, 2004, **375**, 39–43.
11 D. Y. Li, Y. X. Wang, X. R. Zhang, G. Shi, G. Liu and Y. L. Song, *J. Alloys Compd.*, 2013, **550**, 509–513.
12 Y. N. Zhu, G. H. Zheng, Z. X. Dai, J. J. Mu and Z. F. Yao, *J. Mater. Sci. Technol.*, 2017, **33**, 834–842.
13 Y. Zhu, G. Zheng, Z. Dai, L. Zhang and Y. Ma, *J. Mater. Sci. Technol.*, 2017, **233**, 23–29.
14 F. Chun, B. Zhang, H. Su, H. Osman, W. Deng, W. Deng and W. Yang, *J. Lumin.*, 2017, **190**, 69–75.
15 T. Thongtem, A. Phuruangrat and S. Thongtem, *Mater. Lett.*, 2008, **62**, 454–457.
16 H. C. Lei, X. B. Zhu, Y. P. Sun and W. H. Song, *J. Cryst. Growth*, 2008, **310**, 789–793.
17 R. Krishnan, J. Thirumalai, S. B. Thomas and M. Gowri, *J. Alloys Compd.*, 2014, **604**, 20–30.
18 T. Thongtem, S. Kungwankunakorn, B. Kuntalue, A. Phuruangratc and S. Thongtem, *J. Alloys Compd.*, 2010, **506**, 475–481.
19 Y. Sun, J. F. Ma, J. R. Fang, C. Gao and Z. S. Liu, *Inorg. Chem. Commun.*, 2011, **14**, 1221–1223.
20 R. Karthik, N. Karikalan, S. M. Chen, J. V. Kumar, C. Karuppiah and V. Muthuraj, *J. Catal.*, 2017, **352**, 606–616.
21 A. Moghtada and R. Ashiri, *Ultrason. Sonochem.*, 2015, **26**, 293–304.
22 A. Moghtada and R. Ashiri, *Ultrason. Sonochem.*, 2016, **33**, 141–149.
23 J. Zhang, R. Li, L. Liu, L. Li, L. Zou, S. Gan and G. Ji, *Ultrason. Sonochem.*, 2014, **21**, 1736–1744.
24 D. Daniel and I. G. R. Gutz, *J. Pharm. Biomed. Anal.*, 2005, **37**, 281–286.
25 E. Y. Z. Frag, M. A. Zayed, M. M. Omar, S. E. A. Elashery and G. G. Mohamed, *Int. J. Electrochem. Sci.*, 2012, **7**, 650–662.

26 A. Sawa and S. H. Snyder, *Science*, 2002, **296**, 692–695.
27 A. A. Ensafi and E. Heydari, *Anal. Lett.*, 2008, **41**, 2487–2502.
28 H. R. Sobhi, Y. Yamini and R. H. H. B. Abadi, *J. Pharm. Biomed. Anal.*, 2007, **45**, 769–774.
29 C. Sanchez, M. A. Martinez and E. Almarza, *Forensic Sci. Int.*, 2005, **155**, 193–204.
30 B. Danielsson, I. Surugiu, A. Dzgoev, M. Mecklenburg and K. Ramanathan, *Anal. Chim. Acta*, 2001, **426**, 227–264.
31 S. M. Sultan, *Talanta*, 1993, **40**, 681–686.
32 D. Stevenson and E. Reid, *Anal. Lett., Part B*, 1981, **14**, 741–761.
33 M. G. F. Sales, J. F. C. Tomas and S. R. Lavandeira, *J. Pharm. Biomed. Anal.*, 2006, **41**, 1280–1286.
34 Y. Huang and Z. Chen, *Talanta*, 2002, **57**, 953–959.
35 G. Xu and S. Dong, *Anal. Chem.*, 2000, **72**, 5308–5312.
36 F. J. Lara, A. M. G. Campana, F. A. Barrero and J. M. B. Sendra, *Electrophoresis*, 2005, **26**, 2418–2429.
37 Y. Ni, L. Wang and S. Kokot, *Anal. Chim. Acta*, 2001, **439**, 159–168.
38 J. Wang and B. A. Freiha, *Anal. Chem.*, 1983, **55**, 1285–1288.
39 M. H. Parvin, *Electrochem. Commun.*, 2011, **13**, 366–369.
40 M. Karimi, A. H. Mehrjardi, M. M. Ardakani, R. Ardakani, M. Mashhadizadeh and S. Sargazi, *Russ. J. Electrochem.*, 2011, **47**, 34–41.
41 E. Y. Frag, M. A. Zayed, M. M. Omar, S. E. Elashery and G. G. Mohamed, *Int. J. Electrochem. Sci.*, 2012, **7**, 650–662.
42 R. Karthik, Y. S. Hou, S. M. Chen, A. Elangovan, M. Ganesan and P. Muthukrishnan, *J. Ind. Eng. Chem.*, 2016, **37**, 330–339.
43 J. V. Kumar, R. Karthik, S. M. Chen, V. Muthuraj and C. Karuppiah, *Sci. Rep.*, 2016, **6**, 34149, DOI: 10.1038/s41598-017-07423-1.
44 N. Karikalan, R. Karthik, S. M. Chen, M. Velmurugan and C. Karuppiah, *J. Colloid Interface Sci.*, 2016, **483**, 109–117.
45 G. Xing, Y. Li, Y. Li, Z. Wu, P. Sun, Y. Wang, C. Zhao and G. Wu, *Mater. Chem. Phys.*, 2011, **127**, 465–470.
46 Y. Yan, Y. Yu, D. Wu, Y. Yang and Y. Cao, *Nanoscale*, 2016, **8**, 949–958.
47 Z. Xu, Z. Li, X. Tan, C. M. B. Holt, L. Zhang, B. S. Amirkhiz and D. Mitlin, *RSC Adv.*, 2012, **2**, 2753–2755.
48 Y. Lei, J. Li, Y. Wang, L. Gu, Y. Chang, H. Yuan and D. Xiao, *ACS Appl. Mater. Interfaces*, 2014, **6**, 1773–1780.
49 I. Svancara, K. Kalcher, A. Walcarius and K. Vytras, *Electroanalysis with Carbon Paste Electrodes*, CRC Press, Taylor & Francis Group, Boca Raton, FL, 2012.
50 A. A. Ensafi, M. Taei, T. Khayamian, H. K. Maleh and F. Hasanpour, *J. Solid State Electrochem.*, 2010, **14**, 1415–1423.
51 A. Hajian, A. A. Rafati, A. Afraz and M. Najafi, *J. Electrochem. Soc.*, 2014, **161**, B196–B200.
52 D. Bouchta, N. Izaoumen, H. Zejli, M. E. Kaoutit and K. R. Temsamani, *Biosens. Bioelectron.*, 2005, **20**, 2228–2235.
53 B. B. Petkovic, D. Kuzmanovic, T. Dimitrijevic, M. P. Krstic and D. M. Stankovic, *Int. J. Electrochem. Sci.*, 2017, **12**, 3709–3720.
54 M. H. Parvin, *Electrochem. Commun.*, 2011, **13**, 366–369.
55 S. Ahmadzadeh, F. Karimi, N. Atar, E. R. Sartori, E. F. Mirzaei and E. Afsharmanesh, *Inorg. Nano-Met. Chem.*, 2017, **47**, 347–353.
56 N. Zimova, I. Nemec and J. Zima, *Talanta*, 1986, **33**, 467–470.
57 S. Dermis and I. Biryol, *Analyst*, 1989, **114**, 525–526.